



Transfers from Earth to LEO and LEO to interplanetary space using lasers

Claude R. Phipps, Christophe Bonnal, Frédéric Masson, Michel Boustié, Laurent Berthe, Matthieu Schneider, Sophie D Baton, Erik Brambrink, Jean Marc Chevalier, Laurent Videau, et al.

► To cite this version:

Claude R. Phipps, Christophe Bonnal, Frédéric Masson, Michel Boustié, Laurent Berthe, et al.. Transfers from Earth to LEO and LEO to interplanetary space using lasers. *Acta Astronautica*, 2018, 146, pp.92-102. 10.1016/j.actaastro.2018.02.018 . hal-02162240

HAL Id: hal-02162240

<https://hal.science/hal-02162240>

Submitted on 21 Jun 2019

HAL is a multi-disciplinary open access archive for the deposit and dissemination of scientific research documents, whether they are published or not. The documents may come from teaching and research institutions in France or abroad, or from public or private research centers.

L'archive ouverte pluridisciplinaire **HAL**, est destinée au dépôt et à la diffusion de documents scientifiques de niveau recherche, publiés ou non, émanant des établissements d'enseignement et de recherche français ou étrangers, des laboratoires publics ou privés.

Transfers from Earth to LEO and LEO to interplanetary space using lasers

Claude R. Phipps^{a,*}, Christophe Bonnal^b, Frédéric Masson^b, Michel Boustie^c, Laurent Berthe^d,
Matthieu Schneider^d, Sophie Baton^e, Erik Brambrink^e, Jean-Marc Chevalier^f, Laurent Videau^g,
S  verine A.E. Boyer^h

^a Photonic Associates, LLC, Santa Fe, NM, 87508, USA

^b CNES, Direction des Lanceurs, 52 Rue Jacques Hilair  t, 75612, Paris Cedex, France

^c CNRS-Universit   Poitiers, Poitiers, France

^d CNRS-Arts et Metiers ParisTech, Paris, France

^e LULI, CNRS-  cole Polytechnique, Palaiseau, France

^f CEA, DAM, CESTA, Paris, France

^g CEA, DAM, DIF, Paris, France

^h Mines ParisTech, CEMEF PSL, Paris, France

ARTICLE INFO

Keywords:

Laser ablation
Laser-produced plasma
Ultrashort lasers
Laser space propulsion

ABSTRACT

New data on some materials at 80ps pulse duration and 1057 nm wavelength give us the option of proportionally combining them to obtain arbitrary values between 35 (aluminum) and 800 N/MW (POM, polyoxymethylene) for momentum coupling coefficient C_m . Laser ablation physics lets us transfer to LEO from Earth, or to interplanetary space using repetitively pulsed lasers and C_m values appropriate for each mission. We discuss practical results for lifting small payloads from Earth to LEO, and space missions such as a cis-Mars orbit with associated laser system parameters.

1. Introduction

The physics of small payload transfers from Earth to low Earth orbit (LEO) using laser ablation propulsion concepts, as well as for laser propulsion in space were considered in some detail in earlier work [1], [2]. There are many other applications for this technology in space [3]. We predicted that costs of small-target transfers to LEO using this technique could be far below today's \$10,000/kg with multiple launches per day. Missing from these early reports was data on particular ab materials giving practical values of the mechanical coupling coefficient C_m . The history of photon propulsion begins ninety years ago with Tsander [4], Tsiolkovsky [5] and Oberth [6], leading to today's "solar sails." In 1953, S  nger published his concept for photon rockets [7] well before the invention of lasers.

However, for usefully large forces - for example, enough to counteract gravity or accelerate a several-kg object to orbital speeds in a short time, laser ablation propulsion is more attractive than pure photon propulsion.

Laser ablation propulsion operates, ideally in vacuum, by inducing a jet of vapor and plasma from a target using a laser pulse, which transfers momentum to the target (Fig. 1) [8]. Terminology is explained in more

detail in our review of the field [9].

2. Purpose of this paper

The purpose of this paper is to update the reference [2] analysis of propulsion into low Earth orbit (LEO) by including direct launch from the Earth, and to extend the analysis to interplanetary transfers at much higher velocity using new impulse coupling data we recently obtained. We first briefly review the physics and history of this field, then discuss the two applications. When mission duration is at a premium and laser power is not, we will show that C_m as low as 70 N/MW is a good optimum for getting from LEO to Mars and 100–150 N/MW from ground to LEO.

3. Laser momentum transfer physics

The laser impulse coupling coefficient C_m is the ratio of momentum delivered to a target by an ablation jet to the incident beam energy W for a laser pulse, or of surface pressure to incident intensity,

$$C_m = \frac{mT\delta vT/W}{\frac{1}{4}\delta\mu EvE/\Phi} = \frac{1}{4}p/l \quad (1)$$

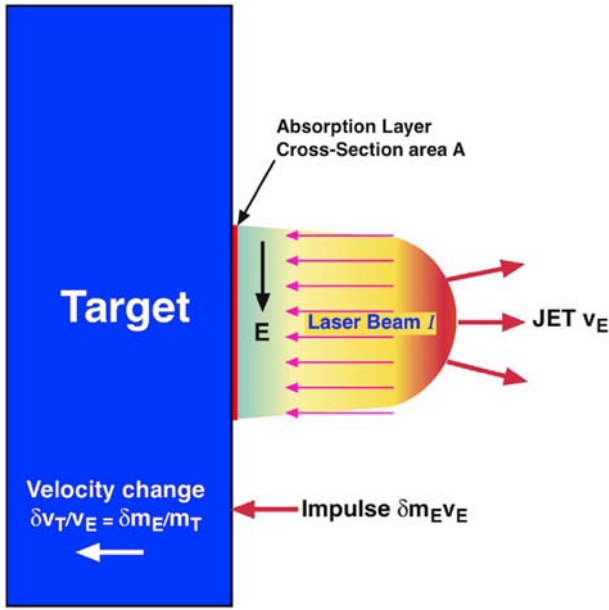


Fig. 1. Impulse from laser ablation.

In Eq. (1), m_T is target mass, p is surface pressure at the target, I is intensity (W/m^2), $\Phi \propto I t$ is fluence on target (J/m^2), v_E is exhaust velocity of the laser ablation jet and δm_E is areal mass density (kg/m^2) in the ablation jet column created by one pulse. C_m has dimensions $\text{N}\cdot\text{s}/\text{J}$ or N/W . C_m for pure-photon pressure is minute: the “momentum coupling coefficient” for pure radiation reflecting off a polished surface is

$$C_m \propto 2/c \propto 6.7 \text{ mN/MW}. \quad (2)$$

A 10-kW laser reflecting perfectly off a surface would produce a thrust of only $67 \mu\text{N}$. The other important parameter for any type of photon propulsion is propellant exit velocity, v_E , simply c for light, but $(2kT_i/m_i)^{1/2} \ll c$ for laser ablation propulsion. T_i and m_i are ion temperature and mass.

Conservation of energy says that the efficiency of the whole process is

$$\eta_{AB} \propto \psi C_m v_E / 2. \quad (3)$$

The parameter $\psi \ll 1$, as we discuss after Eq. (4).

For very long trips, where time is available, solar sails represent a practical use of pure photon propulsion, taking advantage of the fact that, for light in reflection, $I_{sp} \propto c/g_0$, a very large number. The factor of 2 in

the Eq. (2) value for the C_m of light arises from the fact that the energy density of light I/c is doubled on reflection. At $1 \text{ kW}/\text{m}^2$ at our distance from the Sun, a 10-km diameter reflective sail will generate 520 N thrust. Using this thrust, a $2 \mu\text{m}$, 250-ton Al-coated plastic reflective film with this diameter could accelerate to 3 km/s in 17 days. The main problem is how to deploy such a film. Despite decades of development, the largest sail yet deployed (JAXA IKAROS [10], 2010) is $14 \times 14 \text{ m}$.

Variable v_E can be achieved by adjusting laser intensity on target – by changing focal spot area, laser pulse duration and energy – which causes exhaust velocity to vary across the range from chemical reactions (approximately 5 km/s) to much higher values easily reaching 50 km/s. 10,000 K ion temperatures are readily created by a laser pulse. Exhaust velocity is only a matter of intensity [11]. Thrust can be varied independently of v_E by changing the laser pulse repetition rate.

3.1. Ablation propulsion with pulsed lasers

Ablation efficiency is defined as in Eq. (3) where u is drift velocity:

$$\psi \propto \frac{\langle v_x \rangle^2}{\langle v_x^2 \rangle} \propto \frac{u^2}{\langle v^2 \rangle} \propto \frac{u^2}{2kT/m_e} \quad (4)$$

This parameter ψ is the result of the fact that the exhaust velocity distribution is a drifting maxwellian with a nonzero mean velocity. However, it can be shown [12] that high intensity ablation plumes correspond to $\psi \approx 1.15$, and we will assume $\psi \approx 1$ for simplicity in

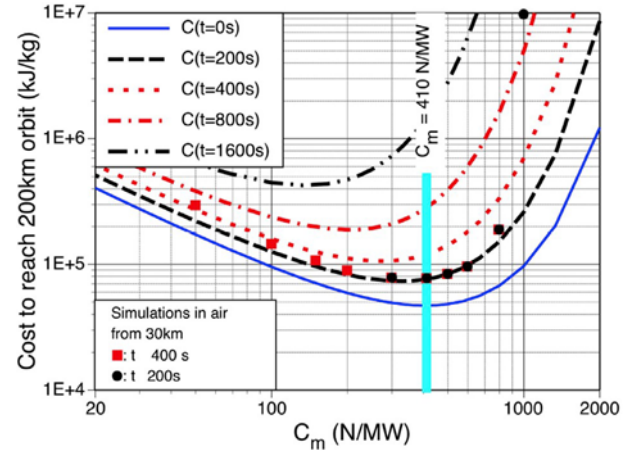


Fig. 3. Results from simulations of laser-powered flights to LEO [2] (with different assumptions than the present work).

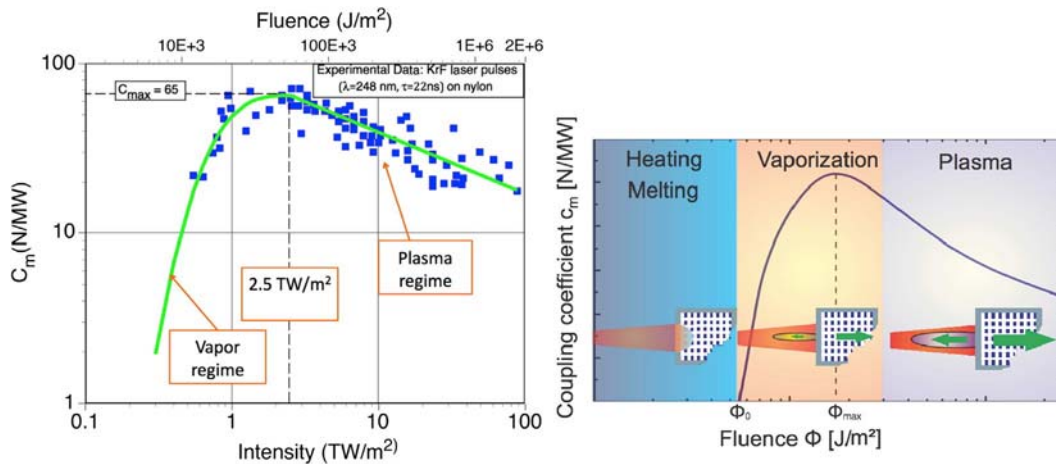


Fig. 2. Illustrating optimum coupling $C_{m, \text{opt}}$ and fluence $\Phi_{\text{opt}} \propto I_{\text{opt}} t$ which occur when parameters are those to produce maximum C_m . Both vapor and plasma regime theory must be considered to find this optimum.

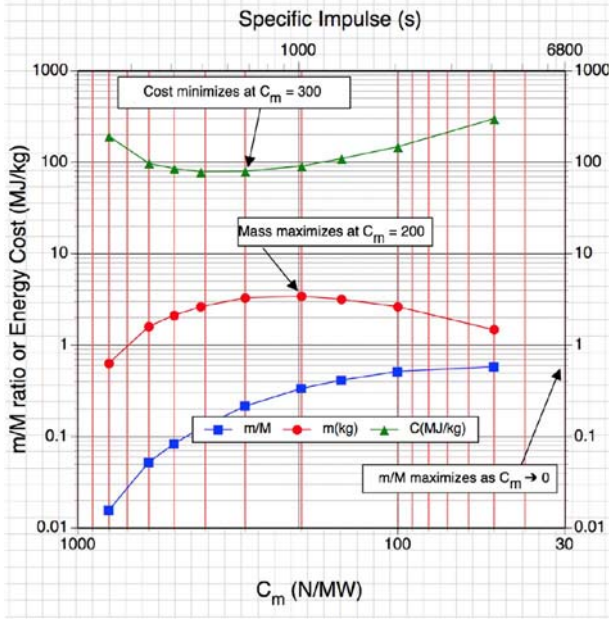


Fig. 4. Simulations in Ref. [2] showed that mass, mass ratio and cost optimize at different values of the coupling coefficient C_m .

Table 1

New laser momentum coupling results (1057 nm).

Material→	Al		POM	
Pulsewidth	C_m (N/MW)	Φ (kJ/m ²)	C_m (N/MW)	Φ (kJ/m ²)
400fs	28 ± 3	50 ± 20	125 ± 12	32 ± 6
80ps	28 ± 3	3.0 ± 7	773 ± 70	40 ± 8

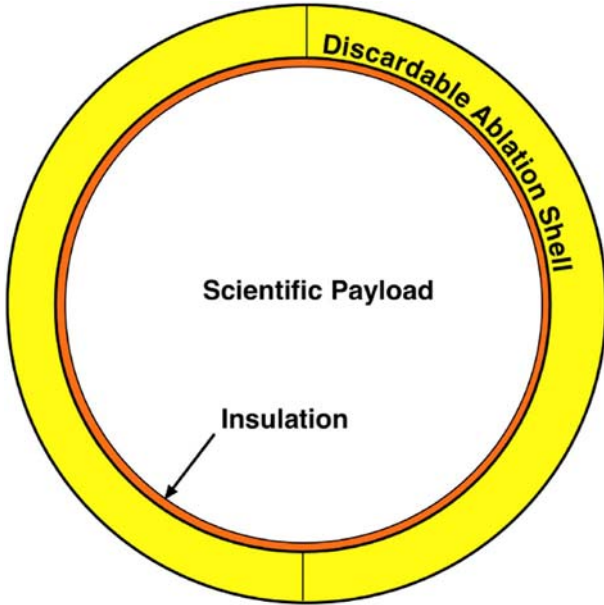


Fig. 5. Laser-propelled flyer.

discussing efficiency. If ψ is larger, Eq. (3) shows it's a bonus for η_{AB} .

The change in velocity of the target from a single pulse is

$$\delta v_T \propto C_m \Phi / \mu_T \quad (5)$$

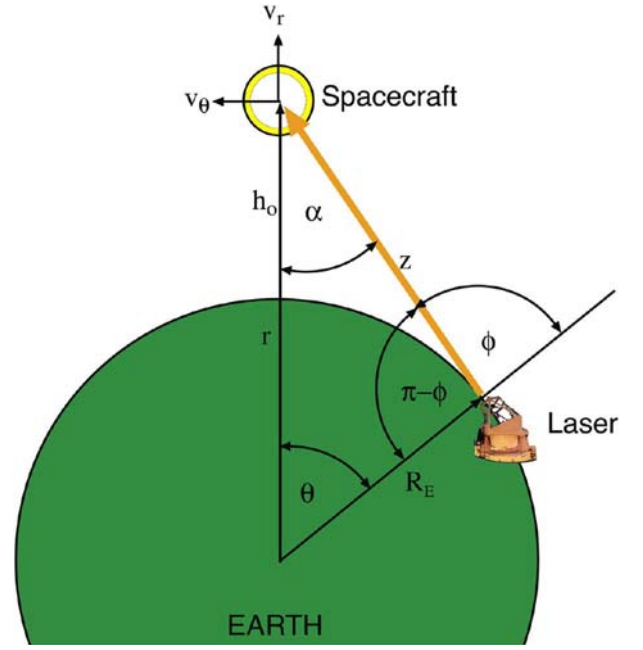


Fig. 6. Geometry for laser launch.

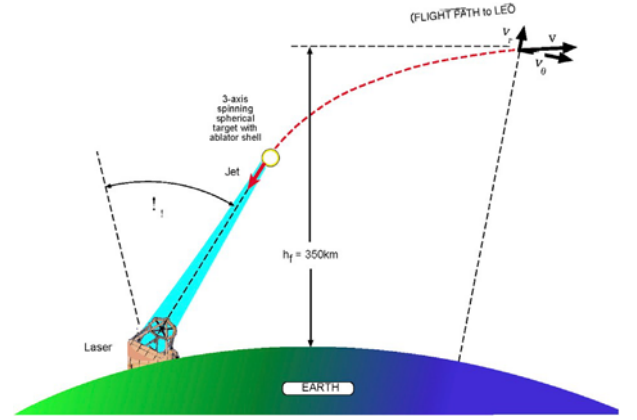


Fig. 7. Laser station inserts the target into orbit. h_f is final altitude.

and

$$\delta v_{Tjj} \propto \eta_c C_m \Phi / \mu_T. \quad (6)$$

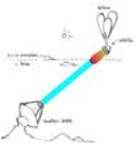



In Eqs. (5) and (6), μ_T is the target's areal mass density, η_c is an average geometrical efficiency factor taking account of the shape of the target and the fact that the ablation jet will be normal to each facet of its surface, not necessarily antiparallel to the laser beam. The quantity δv_{Tjj} is the change in target velocity in the beam direction. Eq. (6) is a numerically convenient formulation for space applications because we can deliver a fluence Φ to a region containing the target and be sure that any object within that region having mass density μ_T and the same C_m will gain the same velocity increment from the pulse. This is valid because space debris tend to exist in families with similar μ_T . For direct comparison to electric propulsion engines, the thrust to electrical power ratio is

$$C_{me} \propto \eta_{eo} C_m. \quad (7)$$

Laser electrical-to-optical efficiency η_{eo} can range from 25 to 80%, depending on the laser type. Exhaust velocity can be determined from the product of the easily measured quantities C_m and Q (J/kg ablated) as follows. Where

Table 2

Ways to achieve initial target altitude above denser part of atmosphere.

Method	Problems	Additional Est. Cost
	Balloon to 35 km <ul style="list-style-type: none"> •Uncontrolled target position at laser turnon •To launch 6 targets, 9900 m³ volume •\$45 k helium cost •Helium is a precious resource 	\$300/kg
	Very large gun <ul style="list-style-type: none"> •1000 G's •Acceleration •Need 1 km/s muzzle velocity •Facility cost dominant •Noise, gov't opposition 	\$200/kg
	Loitering jet plane <ul style="list-style-type: none"> •\$3 k/hr cost •12 km max altitude •4 h/fuel load •8-target load at 50/day •One flight per target 	\$60/kg to 12 km
	Black Brant Rocket <ul style="list-style-type: none"> •\$600 k/launch 	\$2400/kg
	8 km tower <ul style="list-style-type: none"> •Uncertain development cost •Uncertain stability •8 km not enough to help much 	Uncertain
	Laser <ul style="list-style-type: none"> •Combusting target in atmosphere •Penalty on laser energy at lower launch altitude 	Zero additional cost

$$Q \propto W/\delta m_T \propto \Phi/\delta \mu_T, \quad (8)$$

it can be seen dimensionally that the product $C_m Q$ must be velocity:

$$v_E \propto C_m Q. \quad (9)$$

Note that $\delta \mu_T \propto \delta \mu_E$ by mass conservation. Eq. (9) can be extended to show that ablation efficiency is given by

$$\eta_{AB} \propto C_m v_E / (2 \Phi) \propto \frac{C_m}{g_0 I_{sp}} \quad (10)$$

where g_0 is the acceleration of gravity and I_{sp} is the so-called specific impulse. C_m and I_{sp} are a constant product in which I_{sp} varies inversely with C_m for engines with the same efficiency. The units of I_{sp} are seconds. Another constant product is

$$C_m^2 Q / 2 \propto \eta_{AB}. \quad (11)$$

Because $\delta \mu_T \propto \rho_T \delta x$, the thickness of the solid target material ablated

in one pulse is

$$\delta x \propto C_m^2 \Phi / (2 \rho_T \eta_{AB}) \quad (12)$$

and fuel use rate is

$$dm/dt \propto 2 P \eta_{AB} / (g_0 I_{sp})^2 \quad (13)$$

This can equivalently be written

$$dm/dt \propto P C_m^2 / (2 \eta_{AB}) \quad (14)$$

In Ref. [2], we took $\eta_{AB} \propto 1$ for simplicity and because Q (or I_{sp}) were not measured for many materials. This is still true, because these are difficult to measure in single shots.

But we can play a trick: if we write

$$C_m \propto C_{mo} \eta_{AB} \quad (15)$$

and

$$P \propto P_o / \eta_{AB}, \quad (16)$$

Eq. (14) becomes

$$dm/dt \propto P_o C_{mo}^2 / 2 \quad (17)$$

a constant as η_{AB} varies, as is thrust, $F \propto P_o C_{mo}$. The rate of material ablation is very small. As an example, for an aluminum target (density $\rho_T \propto 2700 \text{ kg/m}^3$), if $C_m \propto 70 \text{ N/MW}$, $\Phi \propto 35 \text{ kJ/m}^2$ and $\eta_{AB} \propto 1$, Eq. (12) gives $\delta x \propto 32 \text{ nm}$. At laser repetition frequency $f \propto 50 \text{ Hz}$, even in one minute operation, total ablation depth is $95 \mu\text{m}$. We assume a perfectly uniform beam, such as is achievable with modern methods of apodization.

We note that a consequence of Eqs. (9) and (15) is that the rocket equation for the mass fraction delivered by a flight can be written

$$m/M \propto \exp(-C_{mo} \Delta v / 2), \quad (18)$$

so that especially in space, with a small enough C_{mo} and adequate P_o , almost any mission is possible.

In the laser propulsion examples given in Figs. 8–12 and Table 3, initial laser average power is $5 \text{ MW}/\eta_{AB}$. It increases as η_{AB} decreases, and C_m decreases in the same ratio, so that thrust $F \propto P C_m$ and fuel usage rate are constant. Future measurements will tell us what η_{AB} is.

The laser-produced plasma jet is always perpendicular to the irradiated surface. Temperatures and pressures in plasma that can be achieved by an ultrashort-pulse laser interacting with a target in space range up to 100,000 K and 100 kbar with velocities of several km/s.

3.2. Optima

There are a number of optima to consider in laser propulsion system design. One is the fluence which gives maximum C_m . Fig. 2 shows [13, 14] experimental and notional plots of C_m values vs. incident fluence Φ to illustrate this optimum. In other work, we have called this C_m value and the fluence at which it occurs C_{mopt} and Φ_{opt} .

There is another kind of optimum which gives minimum energy cost to complete a mission. From Fig. 3, it is clear that $C_m \propto 1000 \text{ N/MW}$ had an infinite cost for a 200s flight with the parameters of [2]. For these conditions, Fig. 3 shows that each mission had an optimum-cost impulse coupling coefficient. Lines are theory, dots are simulations for a real atmosphere. Flight time depends on laser power. The purpose of Fig. 4 from Ref. [2] is to illustrate these optima. In Ref. [2], initial masses were 10 and 20.4 kg, and delivered payload mass was 6.1 kg. In the present work, we are not trying to minimize energy expenditure. Instead, we are trying to achieve absolute maximum payload mass fraction delivered at the end of the mission. In Ref. [2], initial mass is 25 kg and delivered mass as large as 13.5 kg. Fig. 4 shows that mass ratio m/M maximizes at $C_m \propto 400 \text{ N/MW}$ [in finite v_E], mass delivered to LEO maximizes at $C_m \propto 200 \text{ N/MW}$ [in $v_E \propto 10 \text{ km/s}$], and cost minimizes at $C_m \propto 300\text{--}400 \text{ N/MW}$. We

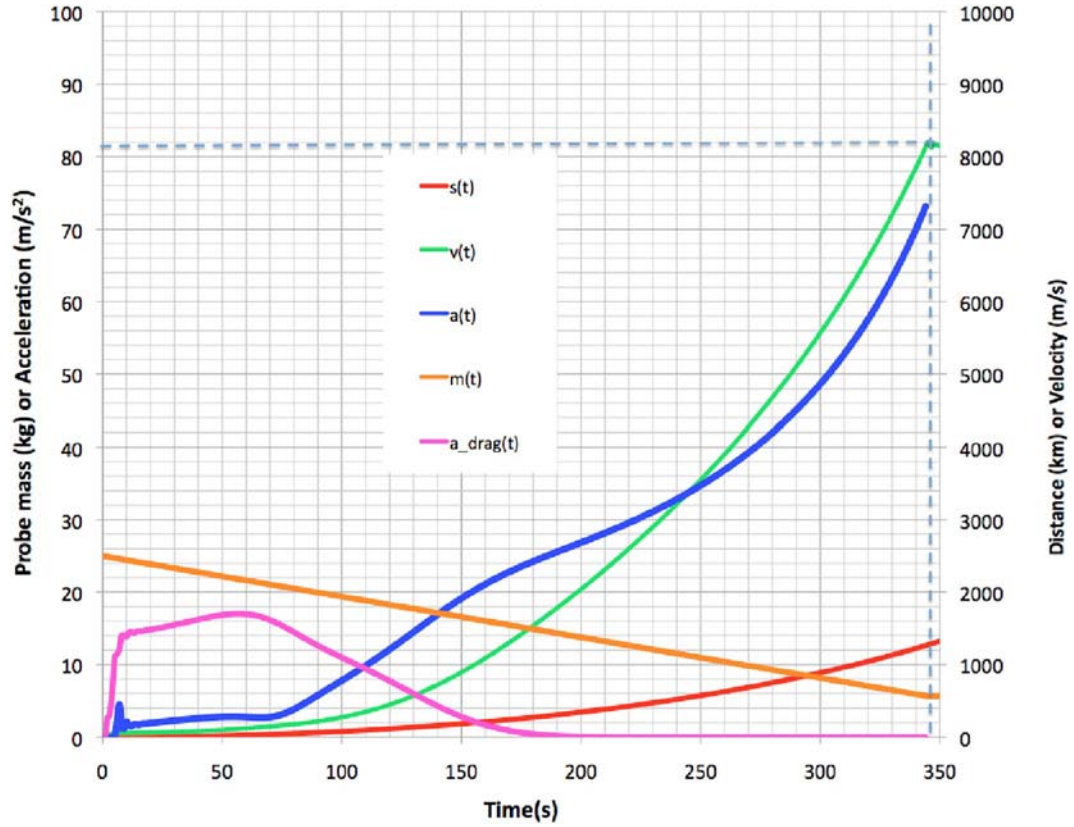


Fig. 8. Case 3. Single power launch from 1 km altitude with $C_m \approx 150$ N/MW. Excessive v_r produces ~ 1.6 km perigee altitude.

assumed $\eta_{AB} \approx 1$ in Ref. [2], so exit velocity is $v_E \approx 2/C_m$. These optima are specific to the ref. [2] case. In Ref. [2], delivered mass ratios were much lower than in the present work because we only considered $P \approx 1$ MW, requiring larger C_m to counteract gravity and smaller zenith angles. Different results are obtained in the present work which involves higher laser power levels. In consequence, more efficiency is reported in this work. Our work in laser propulsion is to find lasers and materials which achieve a desired optimum.

4. DIY coupling coefficient

In experiments conducted at the LULI Laboratory of Ecole Polytechnique [15], we measured C_m on several materials at 400fs and 80 ps, 1057 nm [Table 1]. In the future we will repeat the measurements at 528 nm, which may be more favorable for C_m . For our purposes, the most important results were for Al and POM (polyoxymethylene, Delrin®). The latter material gave very large C_m at 10.6 μm with the Myrabo [16] flyer, which achieved a flight altitude of 72 m in air in 2000 [17]. We found very high C_m for this material at 1057 nm, 80 ps. The same was not true at 400 fs. The POM C_m is too large for most laser launch projects [see Fig. 3], but it is very useful in this way: we now plan to cast ablation fuel from a mixture of Al dust and POM to obtain any value we want in the range from 30 to 770 N/MW at 80 ps. As an example, an Al/POM mixture of 5% POM and 95% Al should give $C_m \approx 70$ N/MW. Density of the combination is 2640 kg/m³, only slightly different from that of Al. The required fluence (~ 30 kJ/m²) is about the same for both materials. For various reasons having to do with available laser hardware at 400 fs, this pulse duration is not attractive compared to 80 ps, so it doesn't concern us that C_{mopt} for POM at 400fs is much less than at 80 ps.

5. Laser launch from Earth to LEO

Fig. 5 shows our notional flyer design, both for launch to LEO and for

interplanetary travel (next section). Diameter is 50 cm. The craft is launched spinning about an axis perpendicular to the beam and very slowly precessing, so that all elements of the surface have equal exposure to the laser beam. A small canister and gas jets produce and maintain these rotations during launch. The mass of the insulation and discardable shell holding the ablator is assumed to be 0.5 kg. For the two cases, the ablator shell will have different C_m values and thicknesses. For LEO launch through the atmosphere, as we will see, C_m will be in the range 110–150 N/MW, while for interplanetary travel $C_m \approx 70$ N/MW. As we will show, a craft designed to do both would have two layers: high C_m to get to LEO and low C_m for the interplanetary portion of the flight.

In Ref. [2], our method of laser-launching an object to low Earth orbit (LEO) was to separate the problem into two parts. First, we drove vertically through the atmosphere to altitude h_0 , leaving a vertical velocity v_{ro} . Then, a second laser located at an appropriate distance to satisfy the geometrical constraints applied as much tangential thrust as possible to achieve orbit. This was too complex. Figs. 7 and 8 show the launch geometry for the present work.

5.1. Equations of motion

Figs. 6 and 7 show the geometry for launch from Earth to LEO. Here, we include atmospheric drag in the simulations. Referring to Fig. 6 for the symbols, we note that

$$\cos \alpha \approx (r^2 \sin^2 \theta - R_E^2) / (2rz) \quad (19)$$

and that the tangential force on the spacecraft from incident laser power P is

$$F_\theta \approx PC_m \sin \alpha, \text{ where} \quad (20)$$

$$F \approx PC_m^{1/4} (dm/dt) v_E \quad (21)$$

is the total force.

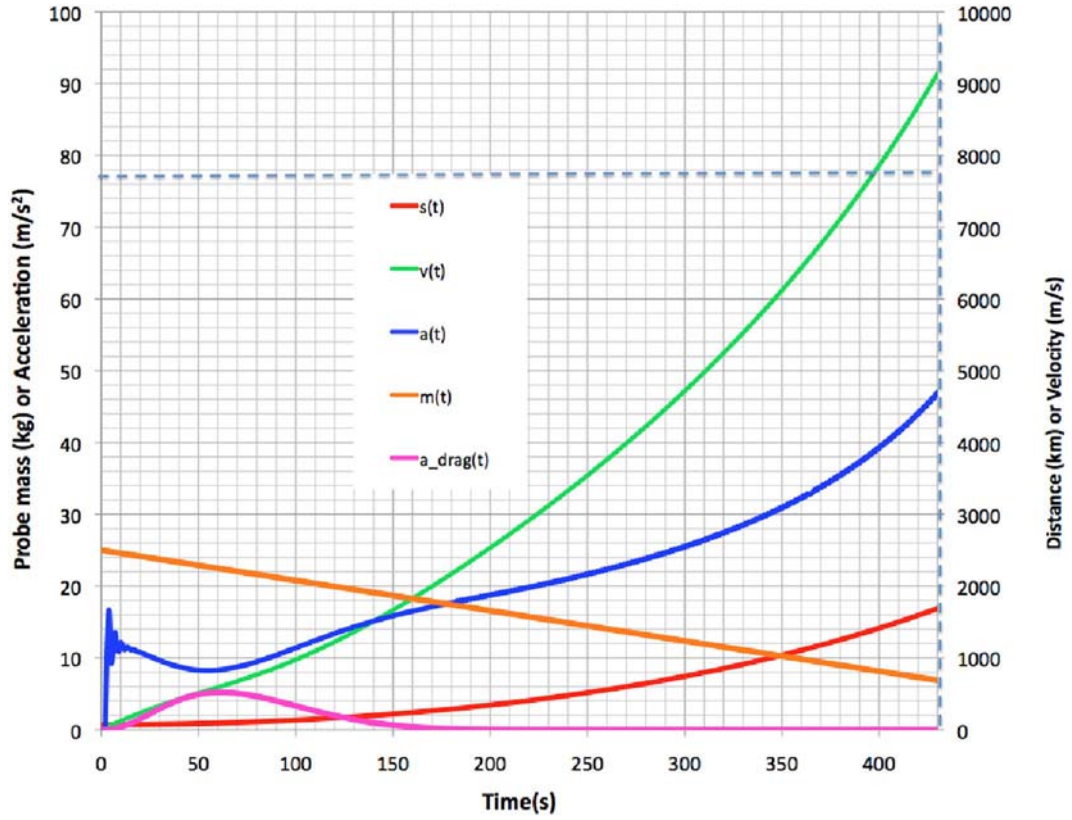


Fig. 9. Case 5. Our only successful single-power laser launch, from 35 km altitude to LEO with $C_m \approx 130$ N/MW. Flight time 429s, laser range $s(t)$. Altitude at insertion is 409 km. Initial zenith angle is 60° and final zenith angle is 90° . Drag loss is significant, mass ratio delivered to orbit 28%. With final radial velocity 1.47 km/s and final velocity 9.09 km/s, vector velocity slope at insertion is barely acceptable (9.3°) for a successful orbit. Perigee 112 km, apogee 10000 km.

Because

$$dL/dt \approx \frac{1}{4} m [r(dv_\theta/dt) + (dr/dt)v_\theta] \approx \frac{1}{4} F_{\theta net} r \approx \frac{1}{4} \text{torque}, \quad (22)$$

dividing by r and including drag,

$$F_{\theta net} \approx \frac{1}{4} (F - C_d A v^2/2) \sin \alpha \approx \frac{1}{4} m (dv_\theta/dt + ((dr/dt)/r)v_\theta), \quad (23)$$

$$\text{And } F_{r net} \approx \frac{1}{4} (F - C_d A v^2/2) \cos \alpha \approx m [\ddot{r} - g_E R_E^2/(R_E + h)^2] \approx m dv_r/dt \quad (24)$$

In Eqs. (19) – (24), $A \approx (\pi D_p^2/4)$ is the exposed cross section area of the spherical flyer, D_p is the flyer diameter, $\rho(h)$ is the atmospheric density – an exponential with scale height 7 km - at altitude h and v^2 is the sum square of the radial and tangential velocities. In Eqs. (19)-(24), all quantities except the obvious constants are functions of time. η_c is a structural efficiency factor to account for the spacial average of the ablation thrust vector, which we take to be 0.8. C_d is the drag coefficient, v_r is vertical velocity, μ is the target areal mass areal density (to match the dimensions of Φ), P is total laser power on target, and f is pulse repetition frequency.

5.2. Initial target altitude and ways to achieve it

The ways we considered are listed in Table 2. Ultimately, we decided the laser itself is the best method vs. balloons, guns, etc.

5.3. Launch strategy

A large number of factors interact to achieve a successful laser launch. Some of these are C_m , flight time, laser range, laser power, delivered mass fraction, final elevation angle, minimum altitude, insertion altitude and laser propagation range. Finding an optimum combination is a matter of art. We found that whatever you do with a laser on the earth's surface, even with the 5–15 MW average power rep-pulse laser which we

used here, it is easy to have the target disappear over the horizon before insertion as well as for it to have an undesirable amount of residual radial velocity. Best performance was obtained with $C_m \approx 120$ –150 N/MW. Compared to the cases discussed in Ref. [2], this choice increases fuel lifetime [see Eq. (17)].

5.4. Flights to LEO

Table 3 and Figs. 8–11 show our results. In our simulations, initial altitudes were chosen as 1, 10, 15 and 35 km. Laser beam range was always < 2000 km. The laser station was assumed to be at 3 km altitude on a mountain so that large zenith angles are more manageable. Acceleration was always modest.

5.4.1. Single phase flight

It is difficult to achieve good flight parameters when laser power is applied continuously. Fig. 8 (case 3 in Table 3) shows a bad example, in which launch from 1 km altitude produces excessive final radial velocity v_{rf} and perigee altitude is negative. Fig. 6 makes it clear why this happens. Even if the flight is initially tangent to the Earth's surface, after a long flight, angle α is no longer $\pi/2$ and an undesirable radial component of thrust exists. A solution is to launch higher.

We were not able to launch from the ground in any single-power flight. In case 3, beginning at 1 km altitude also involved significant loss to drag: delivered mass ratio was 23%. In the Fig. 9 flight (Case 5 of Table 3), we launched from 35 km altitude to minimize energy expended in drag. Even so, only 28% of the mass survived into LEO despite the 35 km launch altitude. To avoid excessive v_{rf} in a single-power flight, the beam elevation angle must be small, leading to high drag in Case 5, and negative perigee in Case 3. The question of how best to get to 35 km still remains (Table 2). This was our only successful single-phase flight.

In Table 3, "Chord" is the horizontal distance from the laser station to

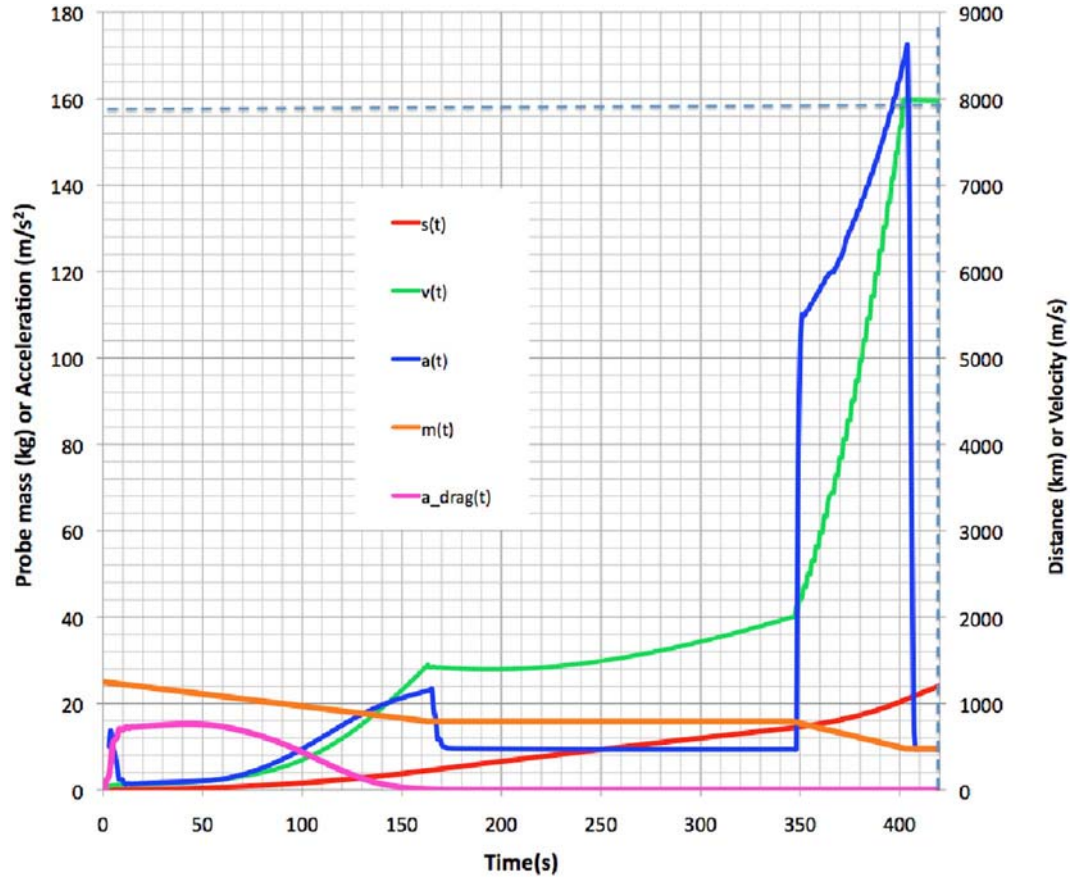


Fig. 10. Case 3A. Laser-launch from 1 km altitude lasting 160 s at 5 MW gets us above the atmosphere quickly. Then, a 180s coast followed by a 10 MW burst in the last 60s gets us into LEO. $C_m \approx 150$ N/MW. Initial zenith angle is 56° , final zenith angle 90° , mass ratio delivered to orbit 38%. Final radial velocity is 238 m/s and final velocity 7.98 km/s. Perigee is 96 km and apogee is 842 km.

the point beneath the satellite at launch. T is flight duration. T_{pkdrag} is the time at which drag is maximized. ϕ_o and ϕ_f are initial and final zenith angles, h_o , h_p and h_a initial, perigee and apogee altitudes, v_{rf} final radial velocity and s_f final laser range to the spacecraft, a_{max} is maximum acceleration, m is mass delivered to orbit and M is mass on the ground.

Perigee and apogee altitudes are assessed using Eqs. (25-28). In Eqs. (25)-(26), μ is the gravitational parameter for Earth (rather than mass areal density), v_f is total velocity, and v_{rf} radial velocity at insertion, $g \approx 9.81$ m/s², and $C \approx 1/4$ (for $v_{rf}/v_f \cos(\phi_f)$), and we have

$$a \approx \frac{1}{4} \left(\frac{2}{r_f} - \frac{v_{rf}^2}{\mu} \right) \quad (25)$$

$$e \approx \frac{1}{4} [1 - C^2 / (\mu a)]^{0.5} \quad (26)$$

$$r_a \approx \frac{1}{4} (1 + e) a \quad (27)$$

$$r_p \approx \frac{1}{4} (1 - e) a \quad (28)$$

5.4.2. Three-phase flight

Now, we use a different technique, in which an initial laser burst gets us above the atmosphere, we coast long enough to develop significant negative radial velocity and then apply a final burst at maximum azimuth angle at 2-3X normal power to achieve orbit with minimum radial velocity. This is called "heat capacity mode operation," in which the laser medium is operated beyond its ability to dissipate heat continuously, for a short time.

Fig. 10 (case 3A) shows results of such a "three-phase flight." Fig. 11 shows that a 45° initial zenith angle is permitted in a three-phase complex flight profile [Table 3, Case 11B]. For this flight, the 41,700 km

apogee with 54% of launch mass delivered suggests applications to inspection of GEO satellites.

5.5. Lasers

Laser parameters assumed in this work are listed in Table 4. Such high repetition rate, high pulse energy lasers are not yet demonstrated, but are being developed. The state of the art in the lasers we currently need to implement these applications is represented in the HiLASE program [18], where the Rutherford Appleton Laboratory's "DIPOLE 100" laser achieved 10 Hz, 100 J pulses at 10 ns pulse duration. Higher repetition rate in this monolithic laser design and higher capacity cooling are needed. Tens of kW are available now in CW fiber lasers, but CW lasers are inappropriate for laser propulsion. Fiber amplifiers give much better heat dissipation, but 100 k pulsed fibers are necessary to generate 100 J pulses [15].

We prefer 1057 nm for the wavelength in atmosphere because absorption is unacceptable at the second and third harmonics, especially at low elevation angles. In space, 355 nm is ideal. For energy storage, 6 GJ, 15 MW super batteries using zinc hybrid cathode technology have now been developed [19]. These batteries can be totally discharged without lifetime penalty. Because 10% discharge/recharge is the rule for most other battery types to ensure long life, this development increases battery mass efficiency by an order of magnitude.

5.6. Discussion

Why are the results here so much better than in Ref. [2]? The main reason is that much larger laser power allows us to oppose gravity with

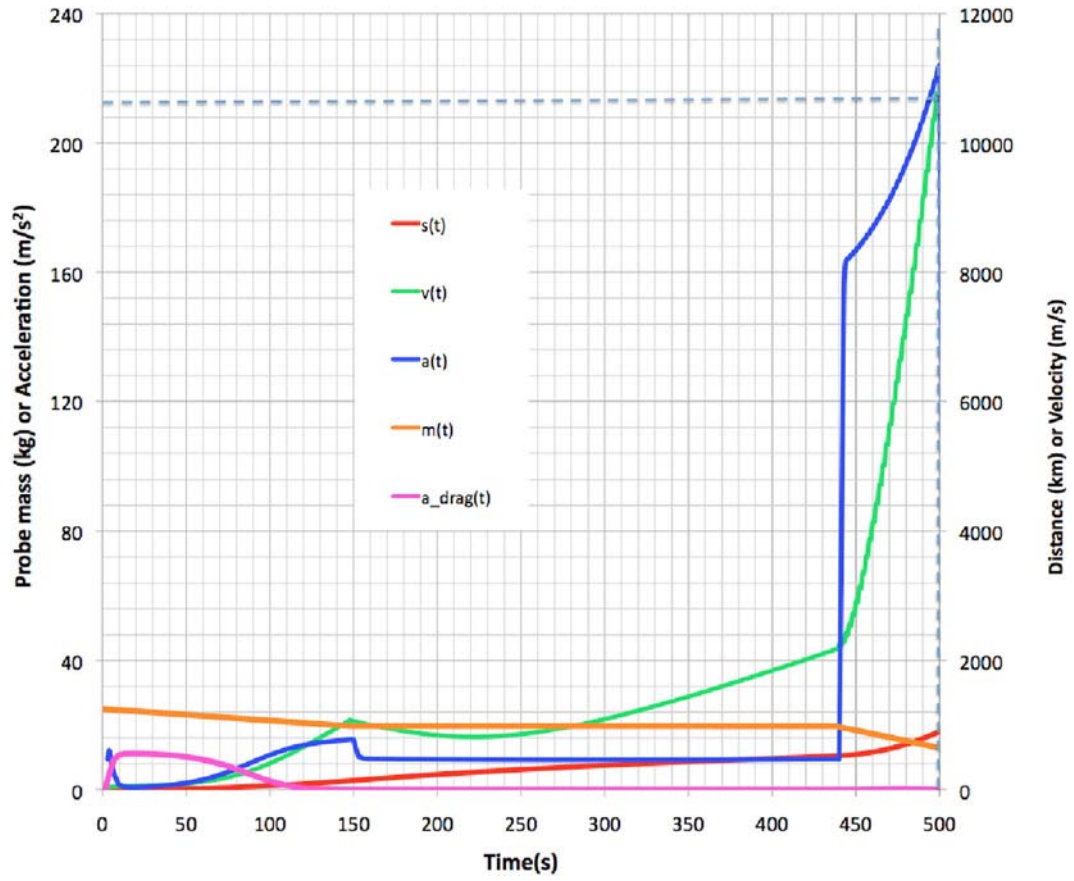


Fig. 11. Case 11B. Fascinating launch from ground (1 km altitude) with $C_m \frac{1}{4}$ 120 N/MW. A 300s coast followed by a 15 MW burst during 60 s at the very end gets our craft into orbit. This profile gives m/M delivered to orbit of 54% (13.5 kg). Initial zenith angle 45.5° , final zenith angle 90° . Final radial velocity is 389 m/s, final velocity 10.4 km/s, perigee 104 km, and apogee 41,700 km, 117% of geosynchronous altitude. Insertion slope is 2.12° . Minimal energy is wasted in drag, even though we are starting from the ground.

Table 3
Launch summary. Common parameter: $P \frac{1}{4}$ 5MW/ η_{AB} . P doubles or triples at end.

Case	C_m/η_{AB} (N/MW)	Chord (km)	T (s)	T pk drag	ϕ_o ($^\circ$)	ϕ_f ($^\circ$)	a_{max} (m/s 2)	v_{rf} (km/s)	m_f/M (%)	h_o (km)	h_p (km)	h_a (km)	s_f (km)
3	150	1.5	344	60	57	84	73	2.87	23	1	-1570	4080	1270
5	130	61	429	55	60	90	47	1.47	28	35	112	10,000	1680
3A	150	1.5	402	60	56	84	173	0.25	38	1	96	842	1030
11B	120	1	496	10	45.5	90	216	0.39	54	1	104	41,700	873

Table 4
Laser and target parameters.

Type	Diode-pumped Nd
Wavelength	1057 nm for ground launch, 532 nm in space
Pulse duration	100ps
Pulse energy	5 kJ
Pulse repetition rate	250 Hz/1kHz/2kHz/3 kHz
Laser average power P_o	1.25–15 MW
Target initial mass m	25 kg
C_{mo}	Various, 70–150 N/MW
D_b (Mirror diameter)	6 m/3 m

smaller C_m , and this leads to better insertion trajectory, higher I_{sp} and longer fuel life [Eq. (13)]. This is because higher temperature gives larger mass velocity in the laser-produced jet. Having 300% of normal power available in a burst at the end of the flight also vastly improves mass delivery, as we show in Table 3. This is our best case for a flight from the ground, with 54% of mass delivered to LEO (1 km starting altitude). Some calculations showed an m/M value of 61% from a 15 km starting

altitude.

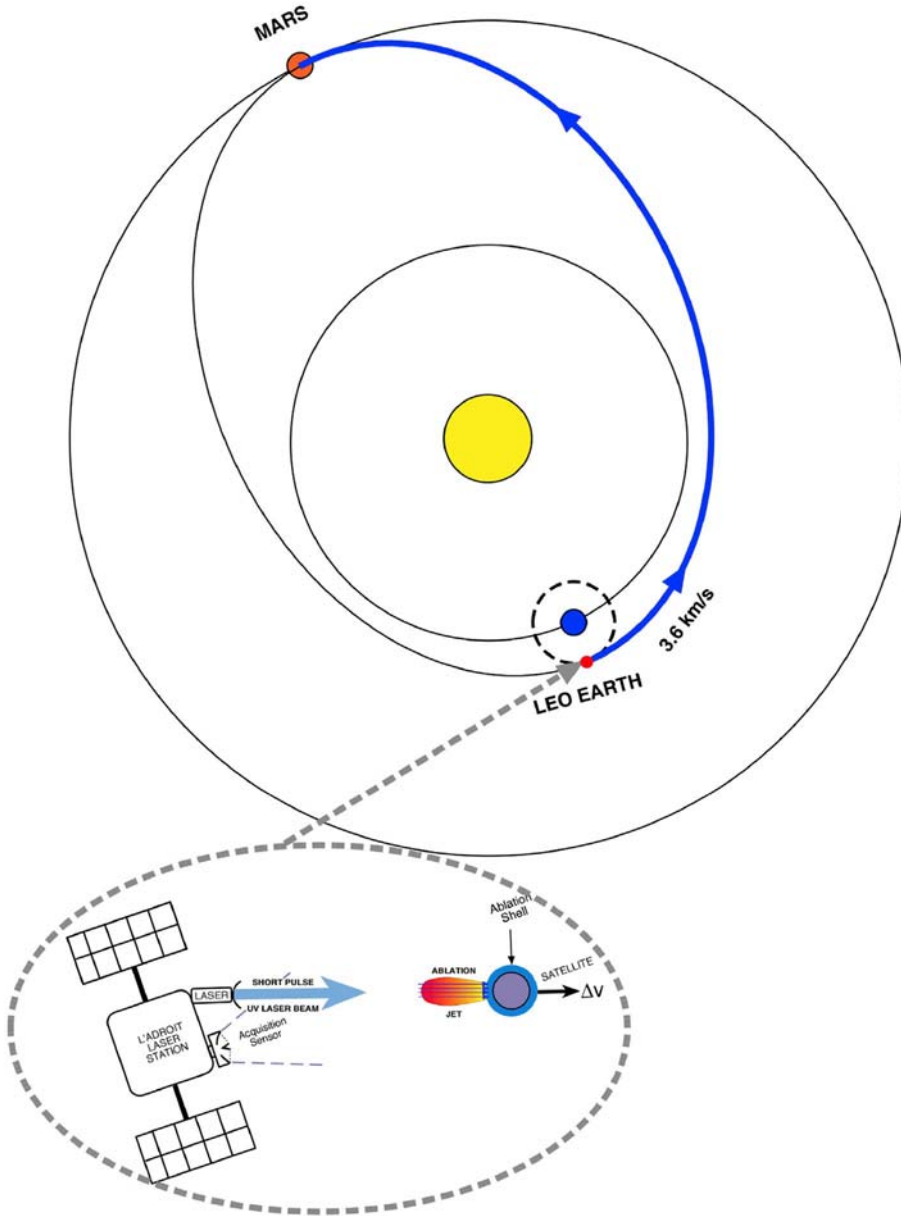
To choose the best flight parameters, there are additional constraints: considering diffraction, scintillation and adaptive optics, maximum permissible range is 2000 km for 1060 nm and a 6-m mirror.

This launch technique can easily reach very large apogees. Delivered mass fraction was very impressive. Contrary to our expectations, launching directly through the atmosphere was possible.

5.7. Energy cost perspective

For the simulations reported in Fig. 5, the minimum emitted laser beam energy cost per kg delivered to orbit was 80 MJ/kg. In case 11B, this cost was 120 MJ/kg. In Ref. [2], we assumed perfect alignment of the beam with the target trajectory, which was supposed to have been achieved with a guidance system and tilting reflectors on the tail of the flyer. In this work, we use a more realistic target that always provides reaction along the beam axis without special mirrors or guidance, but the thrust vector is not perfectly aligned with the path to orbit. This explains the difference in energy cost. The inherent total energy change to create the orbits in Table 3 vary from about 2.4 MJ/kg to 24 MJ/kg. Riding an

Fig. 12. A cis-Mars trajectory starting from LEO requires $\Delta v \approx 3.6$ km/s.



elevator to 150 km amounts to 1.5 MJ/kg. A bullet with 7.98 km/s velocity contains 32 MJ/kg. The parameter Q in Eq. (8) is related to, but incommensurate with, all these values, because it relates to the mass ablated rather than the mass delivered. Q derived from Eq. (11) for a typical flight at 120 N/MW is 140 MJ/kg.

6. Laser-powered rockets

In this section, we consider a laser-propelled rocket, consisting of the Fig. 5 flyer. Flight trajectory is shown in Fig. 12. This is an instantaneous launch, from the point of view of the astrodynamics. Here, we don't have to worry about minimum perigee.

6.1. Equations of motion

The equation of motion in this case is very simple:

$$d^2s/dt^2 \approx \frac{1}{4} P_0 C_{m0} \eta_0 / m \quad (29)$$

because there is no drag. The laser and the target are in a micro-G

environment in LEO, not on the ground. Because an object launched from LEO as shown in Fig. 13 needs a Δv of 3.6 km/s to reach its goal, our only problem is to generate this Δv , rather than worrying about the detailed gravity fields of Earth and the Sun between LEO and Mars. Earth and Sun gravity influence the flight along the way, but all we need to know at the outset is the required Δv and pointing direction, and to deliver it quickly. A flight result is shown in Fig. 13. Mass fraction delivered to Mars is 73%.

6.2. Discussion

The laser-powered rocket is an exciting project for future research. This laser is powered from high performance 6 GJ "super-batteries" [19] which are recharged by solar panels in one day at a 70 kW rate. Laser power is only 1.25 MW, not 5, and can be the third Nd harmonic (355 nm) in space. For this reason the mirror can have 3 m diameter rather than 6 m, as in the LEO launch analysis. Although C_m and I_{sp} have not been measured at 355 nm, theory [ref. (3)] says C_m should be better at the shorter wavelength. We remind the reader that the laser power and C_m values listed in Table 5 should be understood to be adjusted according

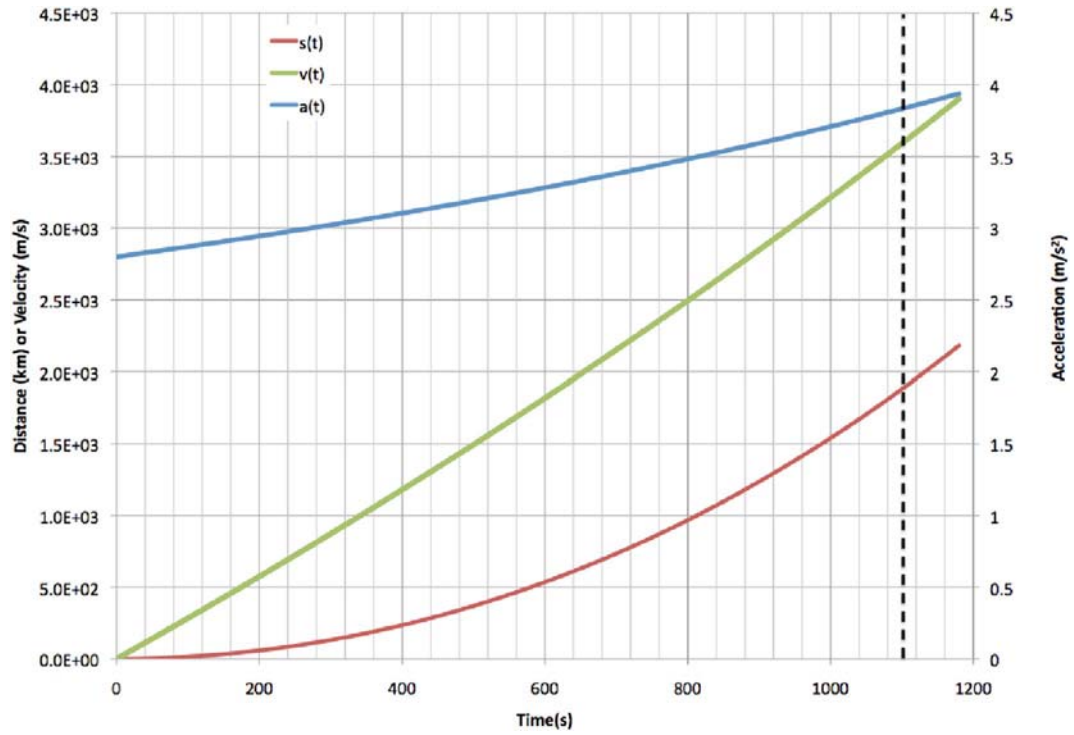


Fig. 13. The necessary velocity of 3.6 km/s is obtained after accelerating for 18.5 min, and 18.2 kg is delivered to the cis-Mars trajectory.

Table 5
Parameters for flight to Mars.

Wavelength (nm)	355
Pulse duration (ps)	100
Pulse energy (kJ)	5
Repetition rate (Hz)	250
Average power (MW)	1.25
$C_m(N/MW)$	70
Fluence Φ (kJ/m ²)	35
Target diameter (cm)	50
Initial mass (kg)	25
Final mass (kg)	18.2 (73%)
Final velocity (km/s)	3.6
Acceleration time (min)	18.5
Mirror diameter (m)	3
Maximum range (km)	1900
Maximum acceleration (m/s ²)	3.84
Ablation efficiency	1.0

to Eqs. (15)–(16) when ablation efficiencies are known. If such a flight were concatenated with a maximally efficient launch from ground to LEO, total mass fraction would be 39% from Earth to Mars, using a combination of groundbased and spacebased lasers. But, that's another paper!

7. Conclusions

For several years, scientists have been launching thin foils with short-pulse lasers to 8 km/s velocities [20]. A way to understand the work reported here is that we launch the equivalent of 400,000 or so thin foils at similar velocities toward the laser beam, one at a time, and the reaction momentum propels a craft in space efficiently.

For the first time, we showed it is possible to laser launch directly from the Earth's surface, and still obtain excellent mass fraction m/M greater than 50% delivered to LEO. This is more than a factor-of-10 improvement over state of the art m/M ratios with chemical rockets. This, an exciting result of this study, can be utilized by assembling larger

stations on orbit from pieces, or for launching swarms of micro- or nanosatellites at low cost.

We used a novel design in which a sphere covered with ablation fuel is caused to rotate randomly so that the entire surface is used for fuel, creating a jet which is always directed opposite to the laser beam. Rotation is presumed to be caused by, e.g., gas jets from a small internal canister. The direction of the beam itself governs the direction of the sphere's trajectory.

These are all passive ablation fuels. As we showed in Ref. [11], it is possible to obtain 3–4 times larger C_m with energetic materials like glycidylazide polymer (GAP).

In the absence of accurate data on specific impulse I_{sp} for our target materials, we showed that it is still possible to use a scaling with laser power inversely proportional to η_{AB} and coupling coefficient C_m proportional to η_{AB} to provide constant thrust and fuel lifetime.

Flight times to LEO were 250–540s. Initial laser power was $5MW/\eta_{AB}$ and the probe initial mass was 25 kg. In the best cases, a burst of 10–15 MW/ η_{AB} was applied in the last 80s, producing a significant increase in m/M as well as a better values for final orbit parameters.

If a practical, low-cost way (balloon, gun, tall tower) is developed to lift the flyers to 15 km before laser acceleration, we showed even better m/M values for the overall flight. The cost of doing this may not be worthwhile. The gains for initiating the flight at 35 km rather than 15 km are probably not worth the additional effort.

Our calculations show that this technology, combined with a 1B\$ groundbased laser station capable of 30 launches/day, can reduce launch costs to LEO to about \$300/kg, a factor of 30 below present experience, because station cost is dominant at high launch rate.

An important application of this work is to launching constellations of Earth-observing microsatellites, to more carefully monitor global climate change and its consequences, in order to spot trends at the earliest possible time and to develop very highly detailed global models. Another application is to sending inspection craft to geosynchronous (GEO) orbit.

The second important result of this work is that it is not difficult to send a probe to Mars in a year or so, with 73% of the mass surviving. Laser wavelength should be the Nd 3rd harmonic in this case (355 nm) because of its better C_m and lower divergence, making possible smaller

mirrors than for the LEO launch case. Maximum laser range was 2000 km.

Further applications of this work are to longer flights within the solar system on one extreme of difficulty, and to placing satellites in LEO or GEO orbits on the other. As higher power lasers are developed, larger masses than 25 kg can also be laser-launched.

Because of Eq. (18), almost any goal can be reached starting from LEO with a sufficiently small C_{mo} , and sufficient laser power.

Acknowledgments

This paper is the written version of Paper no. 679, presented at the

Appendix A. Supplementary data

Supplementary data related to this article can be found at <https://doi.org/10.1016/j.actaastro.2018.02.018>.

Acronyms and abbreviations

Table 6: Acronyms and abbreviations used in this work.

CEA	Commissariat à l'énergie Atomique et aux énergies Alternatives
CEMEF	Centre de Mise en Forme des Matériaux
CESTA	Centre d'Études Scientifiques et Techniques d'Aquitaine
CNES	Centre National d'Études Spatiales
CNRS	Centre National de la Recherche Scientifique
DAM	Direction des Applications Militaires
DIF	DAM Île-de-France
DiPOLE	High repetition rate laser developed by the Rutherford Appleton Laboratory
DIY	Do-it-yourself
GAP	Glycidyl azide polymer
GEO	Geosynchronous orbit
HiLASE	High repetition rate European Union laser project in the Czech Republic
IKAROS	Interplanetary Kite-craft Accelerated by Radiation of the Sun
JAXA	Japan Aerospace Exploration Agency
LEO	Low Earth Orbit
LLC	Limited Liability Corporation
LULI	Laboratoire pour l'Utilisation des Lasers Intenses (École Polytechnique)
Nd	Neodymium lasing medium in glass or other host
POM	Polyoxymethylene, trade name Delrin®

References

[1] C.R. Phipps, M. Michaelis, LISP, *J. Laser Part. Beams* 12 (1) (1994) 23–54.

[2] C.R. Phipps, J. Reilly, J. Campbell, Optimum parameters for laser-launching objects into low earth orbit, *J. Laser Part. Beams* 18 (4) (2000) 661–695.

[3] C.R. Phipps, C. Bonnal, A spaceborne, pulsed UV laser system for re-entering or nudging LEO debris, and re-orbiting GEO debris, *Acta Astronaut.* 118 (2016) 224–236.

[4] F. Tsander, Flight to other planets, in: Ye Moshkin (Ed.), *Development of Russian Rocket Technology*, Mashinostroyeniye Press, Moscow, 1924 (1973) (in Russian).

[5] K. Tsiolkovsky, Plan of Space Exploration, 1926 (in Russian), available in English in "Exploration of the Universe with Reaction Machines: Exploring the Unknown," NASA History Series. NASA SP 4407, Washington, D.C. (1995).

[6] H. Oberth, *Die Rakete zu den Planetenräumen* (The Rocket to the Planet Spaces), Oldenbourg Verlag, München, 1923.

[7] E. Sänger, Zur Theorie der Photonenraketen, Probleme der Weltraumforschung (IV), in: *Internationaler Astronautischer Kongress, Zürich 1953*; S. 32, Laubscher, Biel-Bienne, 1955.

[8] C.R. Phipps, Pulsed lasers for clearing debris in LEO and GEO, paper LSSE1-1, in: *Optics and Photonics International Conference*, Yokohama, 17–20 May 2016, 2016.

[9] C.R. Phipps, M. Birkan, W. Bohn, H.-A. Eckel, H. Horisawa, T. Lippert, M. Michaelis, Y. Rezunkov, A. Sasoh, W. Schall, S. Scharring, J. Sinko, Review: laser ablation propulsion, *J. Propul. Power* 26 (4) (2010) 609–637.

[10] H. Yano, Cosmic dust detection by the IKAROS large area dust detectors ion interplanetary space from the Earth to Venus, in: *42nd Lunar and Planetary Science Conference*, 2011 [in Japanese].

[11] C.R. Phipps, J. R. Luke, W. Helgeson, Laser-powered, multi-Newton thrust space engine with variable specific impulse, in: *High-Power Laser Ablation VII*, *Proceedings of SPIE 7005*, 1X1-1X-8, 2008.

[12] C.R. Phipps, J.R. Luke, Laser space propulsion, in: *Laser Ablation and its Applications*, Chap.16, Springer, 2007, pp. 407–434.

[13] C.R. Phipps, J.R. Luke, D. Funk, D. Moore, J. Glowina, T. Lippert, Laser impulse coupling at 130fs, *Appl. Surf. Sci.* 252 (2006) 4838–4844.

[14] Courtesy of H.-A. Eckel, DLR Stuttgart, 2016.

[15] C.R. Phipps, M. Boustie, J.-M. Chevalier, S. Baton, E. Bambrink, L. Berthe, M. Schneider, L. Videau, S.A.E. Boyer, S. Scharring, Laser impulse coupling and ablated mass measurements at 400fs and 80ps using the LULI facility at 1057nm wavelength, *J. Appl. Phys.* 122 (2017) 193103, <https://doi.org/10.1063/1.4997196>.

[16] L.N. Myrabo, D.G. Messitt, F.B. Mead Jr., Ground and flight tests of a laser propelled vehicle, paper AIAA 98-1001, in: *36th AIAA Aerospace Science Meeting & Exhibit*, 1998, 12-15 January 1998, Reno, NV.

[17] L.N. Myrabo, World record flights of beam-riding rocket lightcraft: demonstration of 'disruptive' propulsion technology, paper AIAA 2001-3798, in: *37th AIAA/ASME/SAE/ASEE Joint Propulsion Conference*, 2001, 8-11 July 2001, Salt Lake City, UT.

[18] HiLASE Project, Czechia, Advanced DPSSL Laser, DiPOLE 100, Delivers 1kW Performance, 2016. <http://www.hilase.cz/en/advanced-dpssl-laser-dipole-100-delivers-1kw-performance/>.

[19] See <https://eosenergystorage.com/products-technology/> for high energy density ZNYTH Zinc Hybrid Cathode Technology.

[20] Z. Gong, et al., Experimental Study for Laser-driven Flyer Plates up to 8km/s, *International Astronautical Federation*, 2015 paper IAC-15, A6.3.8,x29049.

7th European Conference for Astronautics and Space Sciences (EUCASS), Politecnico di Milano, 3–6 July 2017.

The research of my coauthors developing the Table 1 data and exploring a new area in Space Science was partly funded by the CNES through grant AVP-CT-0-1603. The authors thank the LULI Program Committee for having allocated pluriannual beamtime for us to use the ELFIE facility 16TW-F6.

C. R. Phipps benefited immensely from discussions with coauthors, especially Messrs. Bonnal and Masson during development of this topic. C. R. Phipps' work did not receive any specific grant from funding agencies in the public, commercial, or not-for-profit sectors.

C. R. Phipps earned a Ph.D. from Stanford University in 1972 and B.S. and M.S. degrees from the Massachusetts Institute of Technology. He worked at Lawrence Livermore Laboratory and Los Alamos National Laboratory before forming Photonic Associates, LLC in 1995. His interest in laser propulsion goes back to that year.